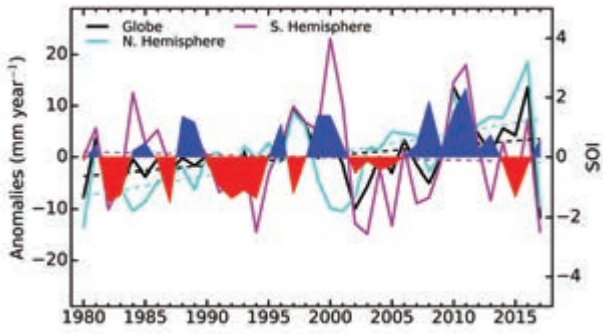

Fig. 2.34. Land evaporation anomaly (mm yr^{-1}; 1980–2017 base period) for the NH, SH, and the entire globe (blue, purple, and black solid lines, respectively). Linear trends in evaporation (dashed lines) and the SOI from NOAA (right axis, shaded area) are also shown. (Source: GLEAM.)

Northern Hemisphere. This trend is qualitatively and quantitatively in agreement with Clausius–Clapeyron expectations in a warming atmosphere (Miralles et al. 2014; Brutsaert 2017). The global average terrestrial evaporation in 2017 was slightly below this trend and close to the 1980–2016 mean (Fig. 2.34). Notwithstanding the novel insights made available from remote platforms, trends in satellite-based evaporation should be interpreted with care, and the weighted use of multiple retrieval approaches is usually recommended (Miralles et al. 2016; McCabe et al. 2016). Unfortunately, as of today, algorithms dedicated to estimating evaporation using satellite observations at global scales are mostly intended for research applications and are not regularly updated in near-real time (Fisher et al. 2017).

e. *Atmospheric circulation*

1) Mean sea level pressure and related modes of variability—R. Allan and C. K. Folland

Overviews of the most recent El Niño have been made in papers such as L'Heureux et al. (2017), but the protracted nature of the El Niño from 2014 to 2016 should also be noted (Allan and D'Arrigo 1999; Allan et al. 2018, manuscript submitted to *Atmosphere*). The climate system exhibited weak La Niña (positive SOI) to neutral conditions following the 2014–16 episode. ENSO, arguably the most globally impactful mode of variability, encompasses a family of events and episodes. Individually, these exhibit wide-ranging effects across the Indo-Pacific region, with teleconnections to higher latitudes in both hemispheres (Capotondi et. al. 2015; C. Wang et. al. 2017). The sea level pressure derived Southern Oscillation index (SOI; Allan et al. 1996; Kaplan 2011) was primarily positive (the phase typically associated with La Niña conditions) from mid-2016 through the end of 2017 (Fig. 2.35). Nevertheless, the immediate impacts of the 2014–16 El Niño episode have lingered in the eastern Australian region, where its influence was particularly profound (Allan and Folland 2017). This has taken the form of persistent above-average eastern Australian SST anomalies from the Coral Sea southwards via major extensions of the East Australian Current into the Tasman Sea region from 2014 through 2017 (Australian Bureau of Meteorology 2017; Oliver et al. 2017). Historically, periods of persistent drought (widespread flooding) in this region have been strongly amplified by protracted El Niño (La Niña) episodes (Murphy and Ribbe 2004; Allan et al. 2018, manuscript submitted to *Atmosphere*).

Mean sea level pressure (MSLP) can also be used to derive indices of many regional modes of variability that drive significant weather and climate events

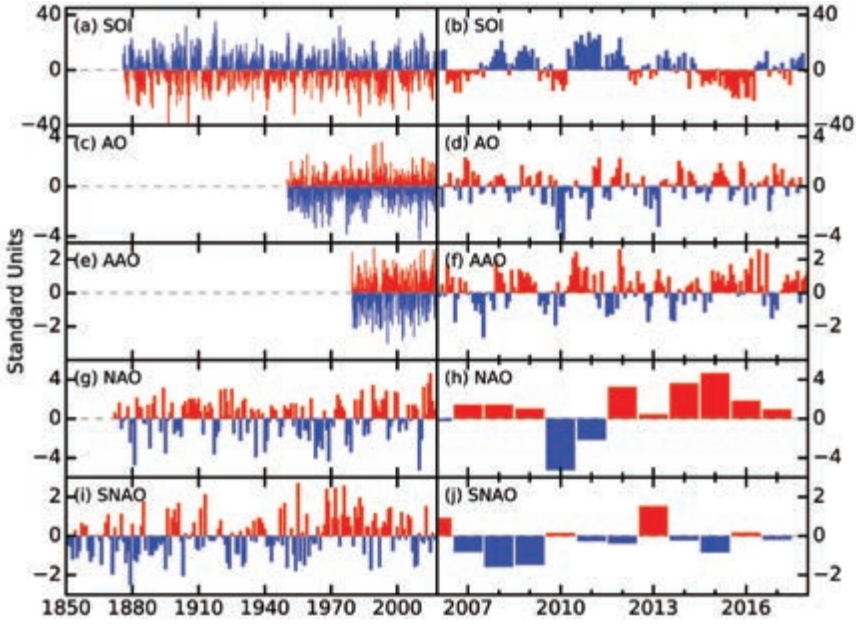

Fig. 2.35. Time series for modes of variability described using sea level pressure for the (left) complete period of record and (right) 2006–17. (a),(b) SOI (provided by the Australian Bureau of Meteorology); (c),(d) AO (NCEP Climate Prediction Center); (e),(f) AAO (NCEP Climate Prediction Center); (g),(h) winter (Dec–Feb) NAO average (NCAR; presented for winter at the beginning of each year so winter 2017/18 is not shown); (i),(j) summer (Jul–Aug) SNAO average (Folland et al. 2009).

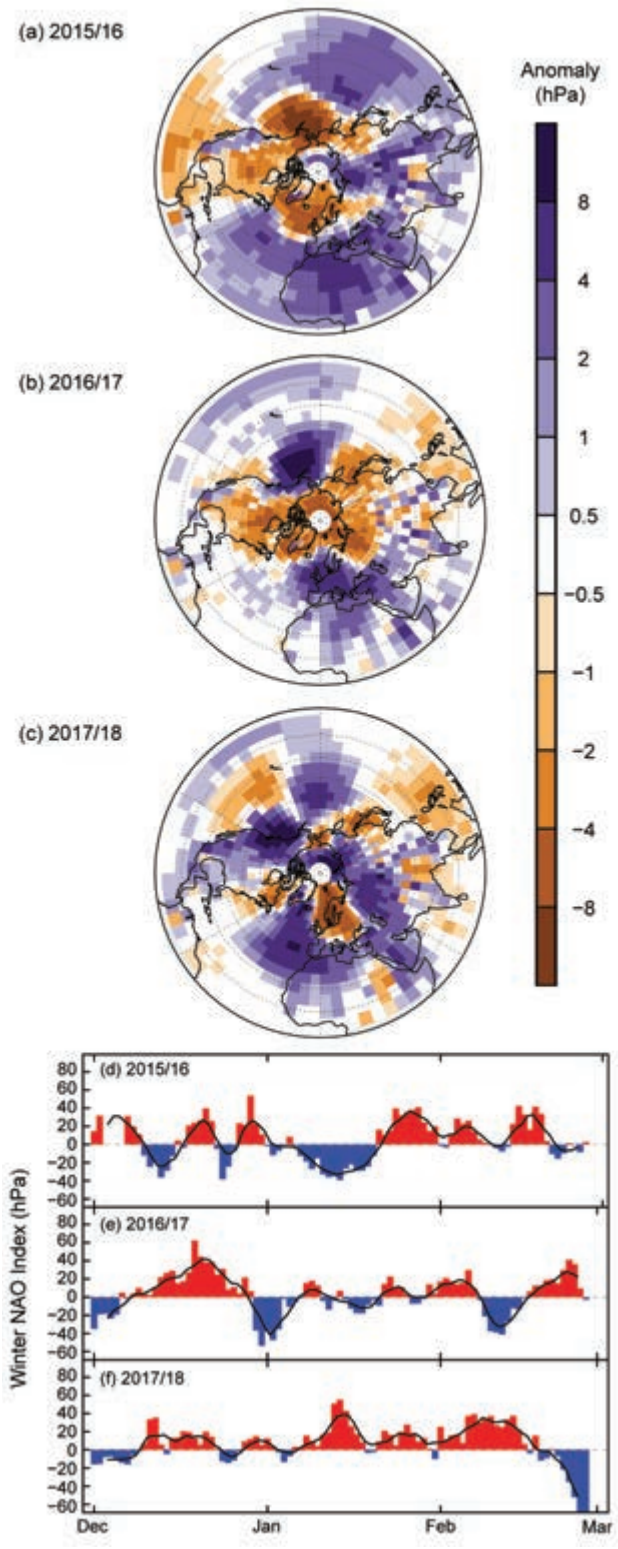

Fig. 2.36. Boreal winter sea level pressure anomalies (hPa; 1981–2010 base period) averaged over Dec–Feb for (a) 2015/16, (b) 2016/17, and (c) 2017/18. NAO daily time series (hPa) for winter (d) 2015/16, (e) 2016/17, and (f) 2017/18. The 5-day running mean is shown by the solid black line. The data are from HadSLP2r (Allan and Ansell 2006).

(Kaplan 2011): the Arctic Oscillation (AO); North Atlantic Oscillation (NAO); summer NAO (SNAO); and the Antarctic Oscillation (AAO) (Fig. 2.35). In the Northern Hemisphere, the last six winters have displayed broadly positive NAO conditions but a diverse range of circulation patterns. During the early winter of 2015/16 the NAO oscillated between phases, with a deep trough over the North Atlantic leading to an enhanced jet stream that directed a series of extratropical cyclones toward northern Ireland and Scotland–northern England (Fig. 2.36). By the mid-to-latter part of the 2015/16 winter the pattern had changed, with the NAO swinging from slightly negative in January 2016 to positive in February 2016 (Allan and Folland 2017). The 2016/17 boreal winter was marked by an increasingly positive NAO through mid-December 2016, temporarily negative NAO values around the start of 2017, and then a fluctuation between phases for the rest of January (Fig. 2.36; Allan and Folland 2017). During the 2017/18 boreal winter, the NAO has been mainly positive (Fig. 2.36). As a consequence, temperatures in Europe were mild to warm, and the region experienced its fifth warmest year on record, while Portugal in particular was strongly impacted, with its driest April to December period in its 87-year record (Section 2d9, Section 7f4). As in 2016/17, the Aleutian low was markedly weakened, leading to reduced rainfall and conditions conducive to major wildfires in the British Columbia region of Canada (Section 2h3; Figs. 2.36a–c; Section 7b1).

In 2017, the phase of the SNAO defined over July and August as in Folland et al. (2009) was on average slightly negative (Figs. 2.37a,b). As in 2016 (Allan and Folland 2017), there was a rather persistent anticyclonic anomaly over southern Greenland in both months, but this was markedly less intense and smaller than in 2016. This feature is normally associated with a negative SNAO. In fact, July (Fig. 2.37a) had a variable and overall negative SNAO as seen in the daily values (Fig. 2.37c). The most notable feature in summer 2017 was a mostly strong negative SNAO that lasted ten days from the end of July into early August. August overall showed a near-neutral SNAO despite the anticyclonic MSLP anomaly over southern Greenland (Fig. 2.37b) and the variable August daily SNAO series. The multidecadal tendency noted in Allan and Folland (2017) toward a more negative SNAO index since 1970 continued to slow. Thus, the average level of the SNAO index in the last five years is near the average observed over 1850–1960 but is considerably more negative than the positive

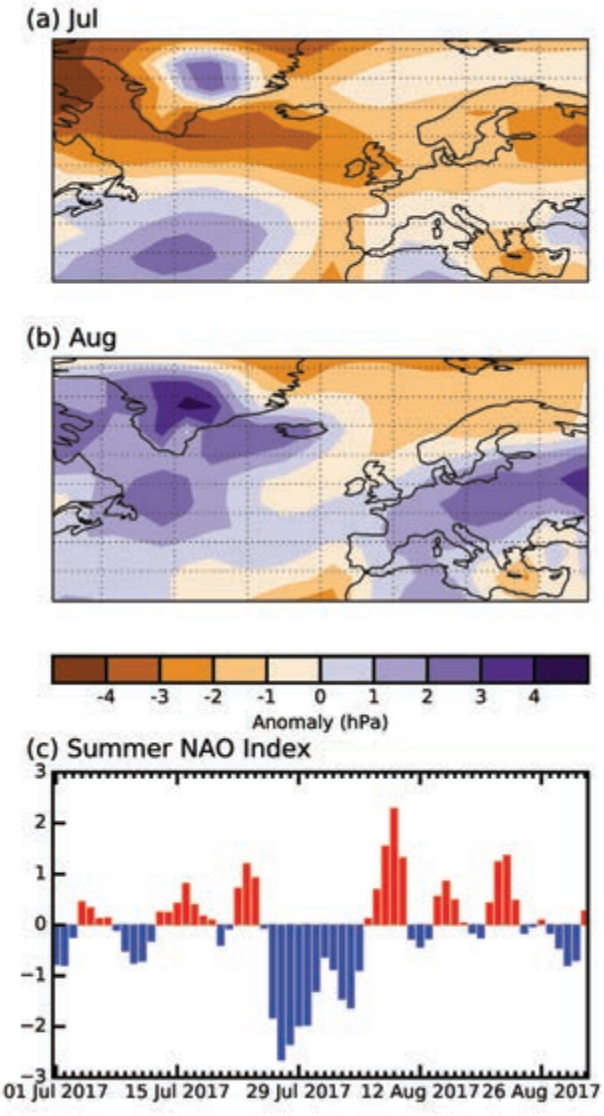

Fig. 2.37. MSLP anomalies (hPa; 1961–90 base period) in (a) Jul and (b) Aug 2017 over the extratropical North Atlantic and Europe. (c) Daily SNAO index for Jul and Aug 2017, calculated from eigenvectors of the daily SNAO.

index averaged over the two decades 1966–1985. Linderholm and Folland (2017) provide more detail on recent multidecadal changes in the SNAO index.

In the Southern Hemisphere, the AAO has been predominantly in its positive phase since 2015/16 (Fig. 2.35). This favors reduced sea ice extent in the West Antarctic Peninsula (WAP) region, owing to enhanced westerly wind conditions (Stammerjohn et al. 2008). In the interplay between the protracted El Niño, which favors a weaker polar jet stream, and a positive AAO mode, with stronger westerly winds, the former appears to have dominated. With the cessation of the protracted El Niño episode in mid-2016 (Allan and Folland 2017; Allan et al. 2018, manuscript submitted to *Atmosphere*), and of a negative AAO (Fig. 2.35), there was a major reduction in the WAP sea ice margin centering on November 2016 and a slight recovery in extent through 2017 (see Section 6e) despite a return to positive AAO values (Fig. 2.35f; http://nsidc.org/data/seaice_index/).

2) Surface winds—C. Azorin-Molina, R. J. H. Dunn, C. A. Mears, P. Berrisford, and T. R. McVicar

Over land, observations of globally averaged wind speed continued to "recover" (commencing in ~2013; Dunn et al. 2016a; Azorin-Molina et al. 2017a) from the previous slowdown of winds (from ~1960s onwards; McVicar et al 2012), termed "stilling" by Roderick et al. (2007). Surface wind speed increased in 2017 (Fig. 2.38a), showing a global (excluding Australia) average wind speed anomaly of +0.024 m s^{-1} with respect to the 1981–2010 climatology (Table 2.4). Regionally, this recent rebound was caused by positive anomalies for central (+0.142 m s^{-1}) and East (+0.108 m s^{-1}) Asia, with Europe (+0.002 m s^{-1}) being very close to average. North America (−0.068 m s^{-1}) showed a negative anomaly but less negative than its 2012 record lowest anomaly. In contrast, Australia

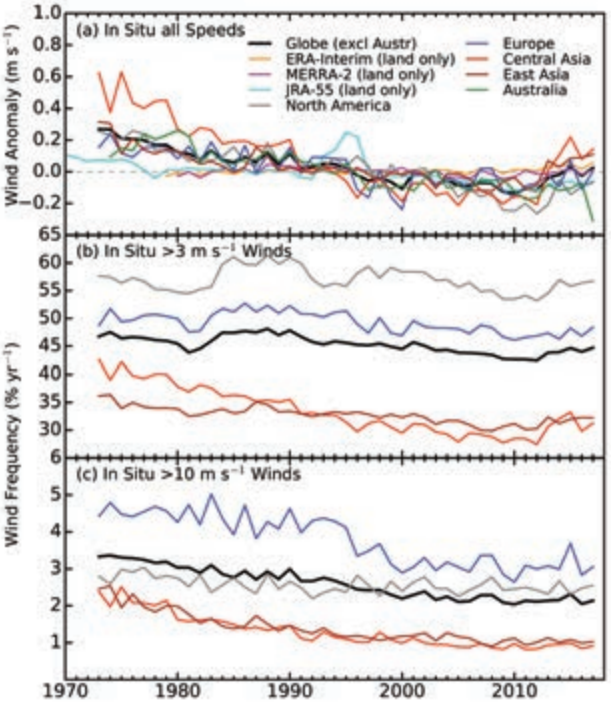

Fig. 2.38. Global (excluding Australia) and regional annual time series of land surface wind speed anomaly (m s^{-1}; relative to 1981–2010) using HadISD2 (1973–2017), an Australian dataset, and ERA-Interim (1979–2017), MERRA-2 (1980–2017) and JRA-55 (1970–2017). Occurrence frequencies (in %) for wind speeds (b) >3 m s^{-1} and (c) >10 m s^{-1} do not include Australia.